

## CT measurements of the proximal femoral medullary cavity in healthy adults: a cross-sectional study

Ran Zhao, Hong Cai, Hua Tian, Ke Zhang

### Abstract

**Objective:** To analyse the proximal femoral morphology on three-dimensional reconstructed imagery to explore the factors influencing the relevant parameters.

**Method:** The cross-sectional study was conducted at Peking University Third Hospital in northern China from January 2019 to August 2020, and comprised healthy adults who underwent computed tomography scanning. Three-dimensional computed tomography reconstruction of the proximal femoral medullary cavity was performed using Mimics 22. The anatomical parameters related to total hip arthroplasty were measured to examine the relationship among gender, age and femoral length. Data was analysed using SPSS 20.

**Results:** Of the 63 adults, meaning 126 hips, 21 (33.3%) were males, meaning 42 (33.3%) hips, and 42 (66.6%) were females, meaning 84 (66.6%) hips. The overall mean age was  $51.5 \pm 23.1$  years (range: 23-68 years). The inflection point of the medullary cavity curved at 5-10mm distal to the lesser trochanteric line. Most horizontal plane parameters significantly differed between men and women ( $p < 0.05$ ), with the mean medullary cavity being wider in men than women. There was a significant difference between the genders in the sagittal anterior-posterior diameter of the canal flare index ( $p < 0.05$ ). Age was negatively correlated with the coronal medial-lateral diameter and coronal lateral diameter of canal flare index. In the coronal and sagittal planes, there was a positive correlation between the metaphysis and diaphysis, and the coronal and sagittal planes were positively correlated with the orthogonal plane.

**Conclusions:** Femoral morphology could be influenced by gender and age. Morphological changes of the proximal femoral medullary cavity were not present in a single plane, but were affected by multiple planes. When the diameter of one plane became larger, its orthogonal plane concomitantly increased.

**Key Words:** Proximal femoral, Morphology, CT measurement, Correlation.

(JPMA 73: 37; 2363) DOI: 10.47391/JPMA.7538

**Submission completion date:** 31-10-2022— **Acceptance date:** 19-08-2023

### Introduction

The success of cementless total hip arthroplasty (THA) depends on a close geometric fit between the prosthesis and bone in order to achieve optimal primary stability and secondary biologic fixation<sup>1</sup>. Intraoperative periprosthetic fracture occurs more often in cementless THA than cemented THA because the operative technique for cementless THA requires more aggressive reaming of the medullary canal and tight fixation of the stem to avoid micromotion between the femoral component and cortical bone<sup>2</sup>. An insufficient prosthesis-bone match may lead to loosening of the prosthesis due to a lack of proximal osseointegration<sup>3,4</sup>. This complication can negatively affect rehabilitation, hospitalisation time, and the cost of treatment. Inadequate fixation can lead to

fracture displacement or non-union, poor bone ingrowth, and aseptic loosening of the femoral stem, ultimately requiring reoperation<sup>5</sup>. Therefore, there is a need for morphological studies of the femoral medullary cavity to improve the fit of the prosthesis in THA.

Most studies evaluating the morphology of the proximal femoral medullary cavity are based on two-dimensional (2D) images<sup>6,7</sup>, which cannot be used to measure the three-dimensional (3D) information of the proximal femoral medullary cavity and acetabulum in detail. There are only a few studies based on 3D computed tomography (CT) images<sup>8</sup>.

The current study was planned to use 3D CT imagery to describe the anatomical morphology of the proximal femoral medullary cavity and the parameter variation interval, and to determine the correlations between proximal femoral medullary cavity parameters and demographic characteristics.

.....  
Department of Orthopaedics, Peking University Third Hospital, Engineering Research Center of Bone and Joint Precision Medicine, Ministry of Education, Beijing, China.

**Correspondence:** Hong Cai. Email: caihong\_76@126.com

**ORCID ID.** >>>

## Patients and Methods

The cross-sectional study was conducted at Peking University Third Hospital in northern China from January 2019 to August 2020. After approval from the institutional ethics review committee of Peking University Third Hospital, the sample was raised. Those included were non-randomised healthy adults with no history of lower limb disease. Those with hip symptoms, such as pain, deformity, abnormal movement, or claudication, hip diseases, such as fracture, osteoarthritis, aseptic avascular necrosis of the femoral head, or developmental dysplasia of the hip, history of lower limb surgery, as well as pregnant and lactating women were excluded.

The coordinating system of the images was reconstructed by the same physician for all the participants. To ensure the repeatability of the system, it was re-established after an interval of 1 month, and the angle between the coronal axes was measured. To ensure the reliability of the measurements of the medullary cavity parameters, all parameters were measured twice by two physicians at 1-month intervals. The intragroup correlation coefficient (ICC) was used to evaluate the measurement reliability.

All the participants underwent 64-slice CT scanning (Discovery 750 HD; GE Healthcare, Madison, WI, United States) using the same projection protocol. The parameters were 120 kV, 80mAs, reconstruction thickness 1.0mm, and interlayer spacing 1.0mm. Each participant was placed in supine position with the lower limbs fixed in a neutral position, fully extended and slightly rotated,

with the toes pointing upward. The lower limbs were fixed, and seat belts were fastened to prevent movement during the CT process. The participants were scanned from the iliac crest to the knee joint. The images were saved as Digital Imaging and Communications in Medicine (DICOM) images<sup>9</sup>.

DICOM data from CT scans were imported into Mimics 22 (Materialise, Leuven, Belgium) for 3D reconstruction. The reconstruction of the femur and medullary cavity was performed with the CT bone module, and the proximal femoral medullary cavity morphology was obtained with Boolean operators, cavity filling, morphology operations, and 3D calculations. The centre of rotation of the femoral head was derived by the fitting of a sphere on the surface of the femoral head. The fit centreline was calculated from the femoral medullary cavity rather than the femoral cortex.

The line connecting the centre point of the medullary cavity at 20mm proximal to the lesser trochanteric line (T-20) and 60mm distal to the lesser trochanteric line (T+60) was used as the approximate central axis of the proximal femoral medullary cavity (Figure 1). The plane perpendicular to the central axis of the proximal femur was defined as the horizontal plane. The plane consisting of the centre point of the fitting sphere of the femoral head and the central axis of the proximal femoral medullary cavity was defined as the coronal plane. The plane perpendicular to the coronal plane and the horizontal plane was defined as the sagittal plane.

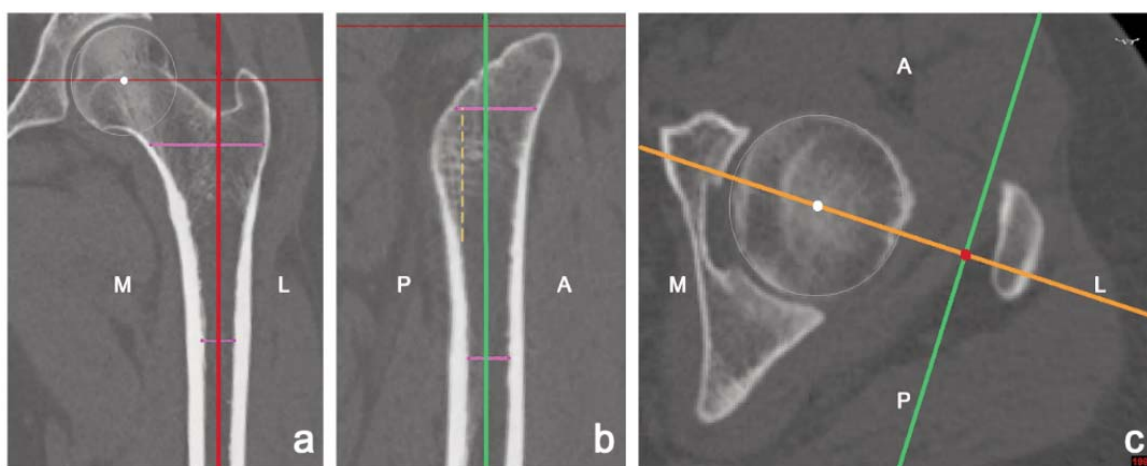


**Figure-1:** Coordinate system reconstruction method. a) Coronal plane through the fitted spherical centre of the femoral head and the axis of the medullary cavity. White dot is the spherical centre of the femoral head. Solid pink line is the coronal medial diameter at 20mm distal to the lesser trochanteric line (MT-20) and at 60mm proximal to the lesser trochanteric line (MT+60). Green line is the projection of the sagittal plane. Red line is the projection of the coronal plane. b) Sagittal plane passing through the central axis of the medullary cavity and perpendicular to the coronal/horizontal plane. Pink solid line is MT-20 and MT+60. Orange dashed line is the coronal plane projection. Red line is the coronal plane projection. Pink dashed line is the demarcation between dense cancellous bone and the medullary cavity. c) Horizontal plane perpendicular to the central axis of the medullary cavity. White dot is the spherical centre of the femoral head. Red dot is the projection point of the central axis of the medullary cavity in the coronal plane. Green line is the projection of the sagittal plane. Orange line is the projection of the coronal plane.

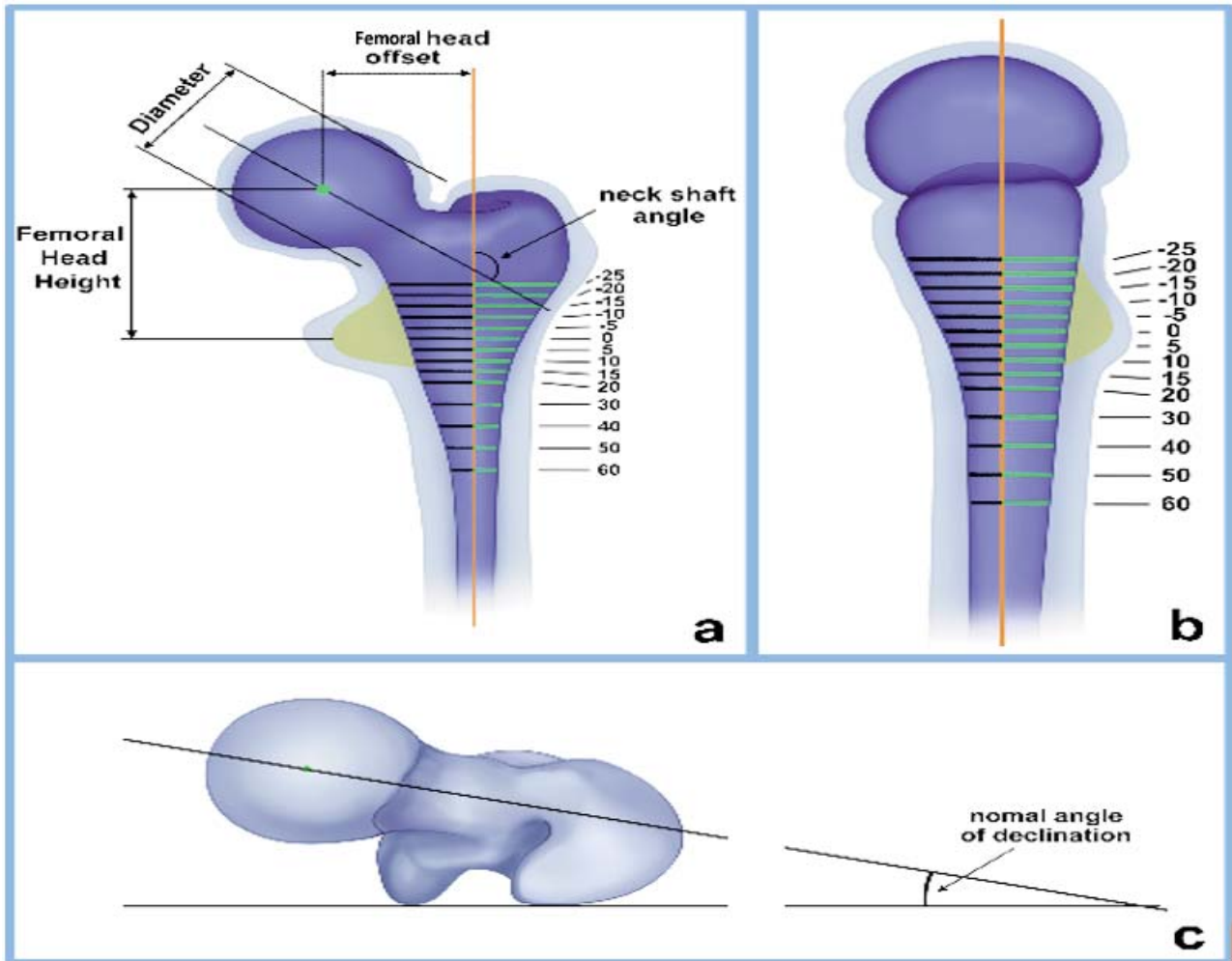


**Figure-2:** Femoral medullary cavity measurement parameters. a) femoral head height (FH), femoral head diameter (FHD) and neck-shaft angle (NSA) Parameters measured in the coronal plane of the femoral medullary cavity. b) Parameters measured in the sagittal plane of the femoral medullary cavity. c) Measurement of the femoral anteversion angle. The yellow region is the cancellous area with high bone density in the inner and posterior endosteal margin of the metaphysis.

The Noble measurement method to describe the medullary cavity morphology<sup>10</sup>. The level of the lesser trochanteric line was set as layer 0 (T). The horizontal plane parameters were then measured every 5mm from the level of 25mm proximal to the lesser trochanteric line (T-25) to the level of 20mm distal to the lesser trochanteric line (T+20), and every 10mm from T+20 to the level 60mm distal to the lesser trochanteric line (T+60) (Figure 2).

The horizontal medullary cavity measurement parameters comprised the coronal medial diameter (M), coronal lateral diameter (L), coronal medial-lateral diameter (ML), sagittal anterior diameter (A), sagittal posterior diameter (P), and sagittal anterior-posterior diameter (AP). M was defined as the distance from the central axis to the medial cortex of the coronal plane. L

was defined as the distance from the central axis to the lateral cortex of the coronal plane. The coronal medial-lateral diameter was defined as M+L of the same section. Further, A was defined as the distance from the central axis to the anterior cortex of the sagittal plane, and P was defined as the distance from the central axis to the posterior cortex of the sagittal plane. The sagittal anterior-posterior diameter was defined as A+P of the same section.

The non-horizontal plane parameters of the proximal femoral medullary cavity were the femoral head offset, neck-shaft angle (NSA), anteversion angle, femoral head diameter (FHD), femoral head height (FH), and femoral length. The canal flare index (CFI60) was calculated as the ratio of T-20 to T+60<sup>11</sup>.

Data was analysed using SPSS 20. Shapiro-Wilk test was used to test data normality. The horizontal plane parameters of the femoral medullary cavity were normally distributed and were tested by the Student's t-test. Partial correlation analysis was used to determine the relationships between anatomical parameters.  $P < 0.05$  was considered statistically significant.

**Results**

Of the 63 adults, meaning 126 hips, 21(33.3%) were males, meaning 42(33.3%) hips, and 42(66.6%) were females, meaning 84(66.6%) hips. The overall mean age was  $51.5 \pm 23.1$  years (range: 23-68 years). The variation of the angle between the coronal axes of the coordinate system was  $< 2^\circ$ , and the ICC of the various indicators varied from 0.83 to 0.94.

The proximal femoral canal diameters of the overall sample were noted (Table 1). Mean ML-CFI60 was  $3.33 \pm 0.62$ , and mean AP-CFI60 was  $2.64 \pm 0.43$ .

The morphology of the medullary cavity of the proximal femur showed that the ML of the medullary cavity gradually narrowed from proximal to distal, and the trend of narrowing gradually decreased, with the narrowing being less obvious at MLT+5 or MLT+10. Also, the M was wider than the L in the metaphysis of the medullary cavity. The A of the medullary cavity gradually narrowed from proximal to distal, and this narrowing was less obvious from APT+5 or APT+10. Moreover, the PT-25 was smaller than PT-20, and tended to be straight from the level of PT-10 to PT+30.

Most horizontal plane parameters significantly differed between men and women, with the mean medullary cavity being wider in men than women (Table 2). Mean ML-CFI60 was  $3.23 \pm 0.82$  for men and  $3.34 \pm 0.52$  for women ( $p = 0.397$ ). There was a significant difference between the genders in the sagittal plane, with AP-CFI60 being significantly greater in men ( $2.42 \pm 0.34$ ) than women ( $2.60 \pm 0.52$  ( $p = 0.020$ )).

**Table-1:** Coronal and sagittal diameters of the femoral medullary cavity.

	ML	M	L	AP	A	P
T-25	$47.53 \pm 5.32$	$29.36 \pm 4.27$	$18.18 \pm 3.15$	$32.14 \pm 4.64$	$21.16 \pm 3.40$	$10.98 \pm 4.53$
T-20	$44.70 \pm 5.08$	$26.64 \pm 4.05$	$18.06 \pm 2.91$	$32.55 \pm 3.72$	$19.15 \pm 3.47$	$13.39 \pm 3.56$
T-15	$39.76 \pm 5.35$	$22.83 \pm 4.30$	$16.93 \pm 2.64$	$25.84 \pm 4.07$	$17.00 \pm 3.15$	$8.45 \pm 3.40$
T-10	$35.32 \pm 4.26$	$19.71 \pm 2.98$	$15.59 \pm 2.42$	$23.98 \pm 5.68$	$15.51 \pm 3.68$	$8.00 \pm 3.06$
T-5	$31.21 \pm 3.95$	$16.91 \pm 2.64$	$14.29 \pm 2.16$	$22.64 \pm 3.91$	$13.86 \pm 2.47$	$8.40 \pm 2.66$
T-0	$27.41 \pm 3.78$	$14.48 \pm 2.46$	$12.93 \pm 2.1$	$20.29 \pm 3.43$	$12.41 \pm 2.16$	$7.74 \pm 2.40$
T+5	$24.67 \pm 3.66$	$12.92 \pm 2.26$	$11.75 \pm 1.87$	$19.69 \pm 4.0$	$11.56 \pm 2.18$	$7.76 \pm 2.39$
T+10	$22.34 \pm 3.23$	$11.52 \pm 1.91$	$10.82 \pm 1.67$	$18.12 \pm 3.21$	$10.78 \pm 1.78$	$7.42 \pm 1.63$
T+15	$20.41 \pm 3.24$	$10.52 \pm 2.11$	$9.89 \pm 1.52$	$17.73 \pm 3.05$	$10.09 \pm 1.74$	$7.63 \pm 1.72$
T+20	$18.92 \pm 2.77$	$9.71 \pm 1.68$	$9.21 \pm 1.39$	$17.13 \pm 2.22$	$9.44 \pm 1.60$	$7.61 \pm 1.31$
T+30	$16.77 \pm 2.50$	$8.46 \pm 1.47$	$8.31 \pm 1.25$	$15.86 \pm 2.76$	$8.40 \pm 1.69$	$7.46 \pm 1.41$
T+40	$15.34 \pm 2.27$	$7.63 \pm 1.32$	$7.71 \pm 1.12$	$14.33 \pm 2.47$	$7.84 \pm 1.27$	$6.49 \pm 1.47$
T+50	$14.35 \pm 2.09$	$7.01 \pm 1.22$	$7.34 \pm 1.03$	$13.39 \pm 2.44$	$7.36 \pm 1.39$	$6.03 \pm 1.34$
T+60	$13.64 \pm 2.10$	$6.67 \pm 1.25$	$6.98 \pm 1.00$	$13.07 \pm 2.50$	$7.25 \pm 1.33$	$5.83 \pm 1.32$

ML: Medial-lateral, M: Medial, L: Lateral, AP: Anterior-posterior, A: Anterior, P: Posterior.

**Table-2:** Gender comparisons of coronal and sagittal horizontal parameters.

Horizontal plane	ML-Male	ML-Female	P	AP-Male	AP-Female	P
T-20	$47.87 \pm 4.69$	$43.13 \pm 4.48$	$< 0.001$	$34.21 \pm 4.63$	$31.62 \pm 3.04$	0.001
T-0	$29.32 \pm 3.83$	$26.43 \pm 3.41$	0.001	$21.44 \pm 3.39$	$19.68 \pm 3.31$	0.019
T+20	$20.68 \pm 2.42$	$18.02 \pm 2.47$	$< 0.001$	$18.21 \pm 2.32$	$16.53 \pm 1.92$	$< 0.001$
T+60	$14.72 \pm 2.23$	$13.12 \pm 1.89$	0.001	$14.43 \pm 2.39$	$12.39 \pm 2.33$	$< 0.001$

ML: Medial-lateral, AP: Anterior-posterior.

**Table 3:** Overall and gender-based values of non-horizontal parameters.

	Total	Male (n=42)	Female (n=84)	P value
<b>Femoral length</b>	382.03±27.92	402.69±28.13	371.79±21.62	0.048
<b>Anteversión</b>	14.23±8.02	13.92±8.28	14.33±7.86	0.671
<b>Offset</b>	40.02±4.36	41.67±3.59	39.22±4.58	0.975
<b>FH</b>	45.02±6.92	46.03±6.40	44.52±7.21	0.293
<b>FHD</b>	43.83±4.07	43.62±5.19	43.82±3.28	0.765
<b>NSA</b>	129.27±5.26	128.69±6.21	129.58±4.82	0.987

FH: Femoral head height, FHD: Femoral head diameter, NSA: Neck-shaft angle.

**Table-4:** Correlations between horizontal plane parameters.

R value	APT-20	MLT-0	APT-0	MLT+20	APT+20	MLT+60	APT+60
<b>MLT-20</b>	0.425**	0.692**	0.484**	0.610**	0.370**	0.267**	0.269**
<b>APT-20</b>	-	0.423**	0.541**	0.424**	0.613**	0.424**	0.505**
<b>MLT-0</b>	-	-	0.518**	0.770**	0.551**	0.428**	0.231*
<b>APT-0</b>	-	-	-	0.442**	0.498**	0.229*	0.231*
<b>MLT+20</b>	-	-	-	-	0.642**	0.730**	0.586**
<b>APT+20</b>	-	-	-	-	-	0.518**	0.596**
<b>MLT+60</b>	-	-	-	-	-	-	0.662**

ML: Medial-lateral, AP: Anterior-posterior.

Except for the femoral length, there was no significant difference between the genders in the parameters of the non-horizontal plane of the femoral morphology, while the mean femoral length was longer in men than women (Table 3).

For the horizontal parameters, age was positively correlated with APT-20 ( $r=0.455$ ,  $p=0.020$ ), PT-20 ( $r=0.533$ ,  $p=0.005$ ), and LT-60 ( $r=0.457$ ,  $p=0.019$ ), and negatively correlated with ML-CFI60 ( $r=-0.279$ ,  $p=0.029$ ) and L-CFI60 ( $r=-0.218$ ,  $p=0.003$ ). Age was not correlated with the non-horizontal parameters ( $P>0.05$ ).

In the coronal plane, there were positive correlations among T-20, T-0, T+20 and T+60, while similar correlations were seen in the sagittal plane, and, finally, the coronal and sagittal plane parameters were positively correlated with the orthogonal plane parameters (Table 4).

Regarding the correlation between horizontal and non-horizontal plane parameters, The FH was negatively correlated with ML-CFI60 ( $r=-0.334$ ,  $p<0.001$ ) and AP-CFI60 ( $r=-0.288$ ,  $p=0.006$ ). There was a negative correlation of NSA with ML-CFI60 ( $r=-0.352$ ,  $p=0.001$ ) and AP-CFI60 ( $r=-0.300$ ,  $p=0.004$ ).

NSA was negatively correlated with the offset ( $r=-0.646$ ,  $p<0.001$ ), and positively correlated with the FH ( $r=0.478$ ,  $p<0.001$ ). Femoral length was positively correlated with

the offset ( $r=0.324$ ,  $p=0.002$ ), FH ( $r=0.615$ ,  $p<0.001$ ) and FHD ( $r=0.543$ ,  $p<0.001$ ).

## Discussion

In THA, early and long-term stability after implantation depend on the achievement of a close fit between the stem and the proximal femoral medullary cavity; micromotion after implantation promotes fibrous tissue growth rather than osseointegration, and this leads to early postoperative failure<sup>12,13</sup>. It has been proved that metaphyseal, fixed prostheses are biomechanically sound, and minimise stress shielding and disadvantageous bone remodelling<sup>14,15</sup>. Therefore, the use of short stems in primary THA is increasing and has good clinical efficacy<sup>16</sup>. Preoperative CT provides accurate anatomical information of the medullary cavity and provides strong evidence for determining surgical goals, especially in the preoperative design of custom prostheses<sup>17</sup>.

In the process of CT scanning, the position of the patient cannot be completely controlled, even with the most rigid positioning, which often causes asymmetry of the pelvis and makes the calculations inaccurate. In addition, the traditional method of using the coronal or sagittal axis of the CT scan itself as the coordinate system does not coincide with the coordinate system, corresponding to the implant placement during the operation. Therefore,

the current study abandoned the use of the CT coordinate system as the sagittal and coronal planes. Furthermore, as the femur itself has an anterior arch and rotation, the axis of the femoral medullary canal was not straight, although the axis of the proximal femoral medullary cavity was usually approximated with a straight line.

In this regard, certain points were considered. For instance, the plane passing through the centre of the femoral head and the axis of the medullary cavity was used as the coronal plane to measure the shape of the medullary cavity and to guide the design of the prosthetic stem. This was done to restore the central position of the femoral head as much as possible.

Besides, the current study did not strictly use the cortical-medullary cavity for division and measurement. CT imaging showed that the density of metaphyseal cancellous bone in the lesser trochanter and the proximal and posterior medullary cavity was lower than that of cortical bone, but higher than that of the medullary cavity, and the cancellous bone in this area was not removed by intraoperative reaming. Therefore, to attain a better fitting stem design, this cancellous bone area should not be included in the medullary cavity measurements.

Also, as most modern prosthetic stems are short and cannot reach the level of the isthmus, many improved definitions of the CFI have been proposed. Boymans et al. proposed the concept of CFI60 as the medullary diameter at the level of 20mm proximal to the lesser trochanteric line divided by that at the level of 60mm distal to the lesser trochanteric line<sup>11</sup>.

Although research on 3D morphology of the medullary cavity using CT has gradually increased, most studies have focussed on the medial and lateral morphology of the medullary cavity rather than the anterior-posterior diameter<sup>10,18</sup>. The current study showed that the medial metaphysis was substantially larger than other diameters. The current study also described the inflection point of the medullary cavity curve, which is beneficial for stem design.

In the current study, the ML and AP were not symmetrical at the reaming point. The M and A were longer than the L and P, respectively. Under such circumstances, if the medullary cavity was opened at the midpoint, this would often lead to the reaming point being placed anteriorly and medially; thus, the selected reaming point should be as lateral and posterior as possible. Current stem designs have minimal width in the anterior-posterior dimensions, which are not connected to cortical bone. However, as

stem designs become shorter and have more filling geometries within the anterior-posterior direction, like the fit and fill designs, a 3D model may be required. It may be optimal to set the AP of the metaphyseal stem asymmetrically to better match the medullary cavity, and guide the placement of the prosthetic stem, especially in cases with excessive bowing of the femur.

In the current study, men had a longer average femoral length and a wider mean medullary cavity than women. However, there were no significant differences between the genders regarding offset, anteversion, NSA and ML-CFI60. This suggests that men and women can use the same brand of prosthesis, except that men require a larger stem. In the sagittal position, the AP-CFI differed between the genders, suggesting that the stem may be more difficult to insert into the distal part of the medullary cavity in women, leading to an increased incidence of intraoperative fractures. Previous studies have reported differences in femoral medullary cavity anatomy between the genders. Yang et al.<sup>8</sup> showed that compared to females, males had a wider femoral head diameter and ML and AP of the medullary cavity, but a smaller CFI, indicating that the isthmus of the medullary cavity was wider in males than in females.

In the current study, the LT-20 became large and the ML-CFI60 and L-CFI60 decreased with age, which means that the CFI60 decreased with age, mainly due to a gradual transition of the medullary cavity morphology from a champagne glass shape to a chimney shape. Previous research has shown that age affects the morphology of the femoral medullary cavity; with increasing age, the bone cortex becomes thinner, and the medullary cavity at the femoral diaphysis enlarges<sup>11,19,20</sup>. Femoral morphology can significantly impact the postoperative leg length discrepancy and osseointegration of cementless THA, as a lower CFI is more prevalent in the elderly population and increases late periprosthetic fracture rates and stress shielding<sup>21</sup>.

The current study revealed a positive correlation between metaphysis and diaphysis, which means that the morphological changes of the proximal femoral medullary cavity were not present in a single plane, but were instead affected by multiple planes. Furthermore, the coronal and sagittal planes influenced each other, which means that when the diameter of one plane became larger, its orthogonal plane concomitantly increased. The NSA was negatively correlated with the offset, which is important in the process of stem design to avoid leg length discrepancy.

In the present study, the horizontal plane parameters

were positively correlated with the FHD, suggesting that the medullary cavity became wider as the FHD increased. The FHD also increased with femoral length. As the subjects' height increased, the FHD and medullary cavity increased. However, although current THA prosthesis designs have many femoral stem sizes, the size of the femoral head prosthesis is often fixed. This may lead to a mismatch with the original anatomical structure.

The present study has limitations, as all participants were from the Chinese population. Previous literature has demonstrated differences in medullary cavity morphology between Asian and Caucasian races<sup>7</sup>. Besides, the sample size was small, and the oldest participant was only aged 68 years. Thus, the medullary cavity morphology of the very elderly population was not evaluated. Finally, all the participants were healthy individuals, indicating that the findings cannot be generalised to patients with diseases of intracapsular/extracapsular deformity of the hip. However, this was not the aim of the present study.

## Conclusion

Proximal femoral morphology was affected by gender and age, with each parameter showing asymmetric change in relation to gender and age. The morphological changes of the proximal femoral medullary cavity were not present in a single plane, but were instead affected by multiple planes. When the diameter of one plane became larger, its orthogonal plane concomitantly increased.

**Acknowledgement:** We are grateful to Kelly Zammit, BVSc, from Liwen Bianji, Edanz Editing China for editing the English text of the manuscript.

**Disclaimer:** None.

**Conflict of Interest:** None.

**Source of Funding:** The Ministry of Science and Technology, China.

## References

1. Massin P, Geais L, Astoin E, Simondi M, Lavaste F. The anatomic basis for the concept of lateralized femoral stems: a frontal plane radiographic study of the proximal femur. *J Arthroplasty* 2000;15:93-101. doi: 10.1016/s0883-5403(00)91337-8.
2. Nowak M, Kusz D, Wojciechowski P, Wilk R. Risk factors for intraoperative periprosthetic femoral fractures during the total hip arthroplasty. *Pol Orthop Traumatol* 2012;77:59-64.
3. Ishii S, Homma Y, Baba T, Ozaki Y, Matsumoto M, Kaneko K. Does the Canal Fill Ratio and Femoral Morphology of Asian Females Influence Early Radiographic Outcomes of Total Hip Arthroplasty With an Uncemented Proximally Coated, Tapered-Wedge Stem? *J Arthroplasty* 2016;31:1524-8. doi: 10.1016/j.arth.2016.01.016.
4. Cooper HJ, Jacob AP, Rodriguez JA. Distal fixation of proximally coated tapered stems may predispose to a failure of osteointegration. *J Arthroplasty* 2011;26(6 Suppl):78-83. doi: 10.1016/j.arth.2011.04.003.
5. Fishkin Z, Han SM, Ziv I. Cerclage wiring technique after proximal femoral fracture in total hip arthroplasty. *J Arthroplasty* 1999;14:98-101. doi: 10.1016/s0883-5403(99)90209-7.
6. Zhao R, Cai H, Liu Y, Tian H, Zhang K, Liu Z. Risk Factors for Intraoperative Proximal Femoral Fracture During Primary Cementless THA. *Orthopedics* 2017;40:e281-7. doi: 10.3928/01477447-20161116-06.
7. Tang ZH, Yeoh CS, Tan GM. Radiographic study of the proximal femur morphology of elderly patients with femoral neck fractures: is there a difference among ethnic groups? *Singapore Med J* 2017;58:717-20. doi: 10.11622/smedj.2016148.
8. Yang Z, Jian W, Li ZH, Jun X, Liang Z, Ge Y, et al. The geometry of the bone structure associated with total hip arthroplasty. *PLoS One* 2014;9:e91058. doi: 10.1371/journal.pone.0091058.
9. Mantri M, Taran S, Sunder G. DICOM Integration Libraries for Medical Image Interoperability: A Technical Review. *IEEE Rev Biomed Eng* 2022;15:247-59. doi: 10.1109/RBME.2020.3042642.
10. Noble PC, Alexander JW, Lindahl LJ, Yew DT, Granberry WM, Tullos HS. The anatomic basis of femoral component design. *Clin Orthop Relat Res* 1988;1988:148-65.
11. Boymans TA, Heyligers IC, Grimm B. The Morphology of the Proximal Femoral Canal Continues to Change in the Very Elderly: Implications for Total Hip Arthroplasty. *J Arthroplasty* 2015;30:2328-32. doi: 10.1016/j.arth.2015.06.020.
12. Lennon AB, Prendergast PJ. Evaluation of cement stresses in finite element analyses of cemented orthopaedic implants. *J Biomech Eng* 2001;123:623-8. doi: 10.1115/1.1412452.
13. Goodman SB. The effects of micromotion and particulate materials on tissue differentiation. Bone chamber studies in rabbits. *Acta Orthop Scand Suppl* 1994;258:1-43. doi: 10.3109/17453679409155227.
14. Trieb K, Huber D, Sonntag R, Kretzer JP. Finite Element Analysis and Biomechanical Testing of the New MiniMIS Short Stem. *Z Orthop Unfall* 2019;157:188-93. doi: 10.1055/a-0715-2398.
15. Walker PS, Robertson DD. Design and fabrication of cementless hip stems. *Clin Orthop Relat Res* 1988;1988:25-34.
16. Liang HD, Yang WY, Pan JK, Huang HT, Luo MH, Zeng LF, et al. Are short-stem prostheses superior to conventional stem prostheses in primary total hip arthroplasty? A systematic review and meta-analysis of randomised controlled trials. *BMJ Open* 2018;8:e021649. doi: 10.1136/bmjopen-2018-021649.
17. Haddad FS, Garbuz DS, Duncan CP, Janzen DL, Munk PL. CT evaluation of periacetabular osteotomies. *J Bone Joint Surg Br* 2000;82:526-31. doi: 10.1302/0301-620x.82b4.10174.
18. Wuestemann T, Hoare SG, Petersik A, Hofstaetter B, Fehily M, Matsubara M, et al. Bone morphology of the proximal femoral canal: ethnicity related differences and the influence on cementless tapered wedge stem designs. *Hip Int* 2021;31:482-91. doi: 10.1177/1120700019895458.
19. Casper DS, Kim GK, Parvizi J, Freeman TA. Morphology of the proximal femur differs widely with age and sex: relevance to design and selection of femoral prostheses. *J Orthop Res* 2012;30:1162-6. doi: 10.1002/jor.22052.
20. Ruff CB, Hayes WC. Sex differences in age-related remodeling of the femur and tibia. *J Orthop Res* 1988;6:886-96. doi: 10.1002/jor.1100060613.
21. Nishino T, Mishima H, Kawamura H, Yoshizawa T, Miyakawa S, Yamazaki M. Ten-year results of 55 dysplasia hips of hip offset and leg length reconstruction in total hip arthroplasty with cementless tapered stems having a high offset option designed for dysplastic femur. *J Orthop Surg (Hong Kong)* 2020;28:2309499020909499. doi: 10.1177/2309499020909499.